Sizing and Locating Planning of EV Centralized-Battery-Charging-Station Considering Battery Logistics System

Chenke He, Jizhong Zhu, *Fellow, IEEE*, Shenglin Li, Ziyu Chen, and Wanli Wu

***Abstract*—This article investigates the optimal planning of centralized charging and multipoint distribution network that includes centralized battery charging stations (CBCSs) and battery distribution stations (BDSs), which considers the battery logistics system. Based on the analysis of the characteristics of travel chains of swapping electric vehicles (SEVs), a time-space load forecasting model of SEVs is proposed. Then, based on function and characteristic analysis, operation models of CBCS, BDS, and the battery logistics system are built. Afterward, the sizing models of CBCSs and BDSs are established. Then, a double-level planning model of CBCSs considering battery logistics system is proposed. In the first level planning, the sizes and locations of CBCSs and BDSs are planned, and in the second-level planning, the economy of battery logistics company is optimized. Finally, the CPLEX toolbox and the Bellman–Ford algorithm are used to solve the planning model. Taking the actual situation of a certain region as the planning area, the feasibility and effectiveness of the method proposed in this article are verified.**

***Index Terms*—Battery distribution station (BDS), battery logistics system, centralized battery charging station (CBCS), planning, swapping electric vehicle (SEV), time-space load forecasting.**

NOMENCLATURE

A. Abbreviations

EV	Electric vehicle.
CBCS	Centralized battery charging station.
BDS	Battery distribution station.
SEV	Swapping EV.
SPEV	Swapping private EV.
SET	Swapping electric taxis.
BTV	Battery transport vehicle.
SOC	State of charge.
BFA	Bellman-Ford algorithm.

B. Indices and Sets

$\mathbf{CBCS}(j)$	Set of BDSs that are energy supply by CBCS *j*.
$\boldsymbol{\Omega}(j)$	Set of the end nodes which belong to the branch with the same start node *j*.
$\boldsymbol{N}_{\text{Grid}}$	Grid node set.
$\boldsymbol{CS}$	Types set of charging and swapping facilities.
$\boldsymbol{Tra}(k)$	Set of CBCSs supplied by the substation *k*.
$\boldsymbol{S}_{T,n}$	Set of rated transformer capacity.
$\boldsymbol{Z}_{\text{CBCS}}, \boldsymbol{Z}_{\text{BDS}}$	Location set of CBCS, BDS.
$\boldsymbol{R}(i,j)$	Road node set of BTV driving path.
$t, T, \Delta T$	Index, hour numbers per day, unit duration.

C. Parameters

t_0	Swapping time of SPEVs.
l	SPEV daily driving distance.
μ_S, σ_S	Charging EV initial charging time parameters.
μ_D, σ_D	SPEV daily driving distance parameters.
$N_{\text{RP},n}, N_{\text{RP,Total}}$	Population of residential region *n*, whole planning area.
$M_{C,n}, M_{\text{C,Total}}, M_{I,n}, M_{\text{I,Total}}, M_{R,n}, M_{R,\text{Total}}$	Area of commercial region *n*, total commercial region area, industrial area *n*, total industrial region area, residential region *n*, and total residential region area.
$N_{\text{SW},N}$	Rated number of SEVs that can be serviced by a swapper in ΔT.
$P_{\text{SW},N}, P_{\text{CH},N}, P_{\text{SM},N}$	Rated power of swapper, charger, swapping equipment.
E_{SEV}	SEV energy storage capacity.
$\eta_{\text{BDS}}, \eta_{\text{SW}}, \eta_{\text{CBCS}}, \eta_{\text{CHA}}, \eta_{\text{SM}}$	Redundancy coefficient of BDS energy storage, swapper, CBCS energy storage, charger, and battery swapping equipment.
$\eta_{\text{CH}}, \eta_{\text{DI}}$	Energy storage charging and discharging efficiency.
$\text{SOC}_{\text{MAX}}, \text{SOC}_{\text{MIN}}$	Upper, lower limits of energy storage.

Manuscript received October 30, 2021; revised March 4, 2022; accepted April 6, 2022. Date of publication April 19, 2022; date of current version July 19, 2022. This work was supported in part by the National Natural Science Foundation of China under Grant 52177087, and in part by the Natural Science Foundation of Guangdong Province under Grant 2021A1515010419. Paper 2021-TSC-1248.R1, presented at the 2021 IEEE 4th International Electrical and Energy Conference, Wuhan, China, May 28–30, and approved for publication in the IEEE TRANSACTIONS ON INDUSTRY APPLICATIONS by the Transportation Systems Committee of the IEEE Industry Applications Society. *(Corresponding author: Jizhong Zhu.)*

The authors are with the School of Electric Power Engineering, South China University of Technology, Guangzhou 510641, China (e-mail: 1197958177@qq.com; jizhong.zhu@ieee.org; eplishl@mail.scut.edu.cn; epchenzy@mail.scut.edu.cn; epwuwanli@mail.scut.edu.cn).

This article has supplementary material provided by the authors and color versions of one or more figures available at https://doi.org/10.1109/TIA.2022.3168244.

Digital Object Identifier 10.1109/TIA.2022.3168244

$N_{\mathrm{CH,N}}$	Rated number of batteries that can be charged by a charger.
$(X_{\mathrm{Road},n}, Y_{\mathrm{Road},n})$	Road node *n*.
$N_{\mathrm{BTV,CI}}$	Round-trip times of a BTV that completes a battery transport task.
$T_{\mathrm{BTV,MAX}}$	Maximum transportation duration.
$A_{\mathrm{SW}}, A_{\mathrm{CH}}, A_{\mathrm{SM}}, A_S, A_{\mathrm{CBCS,T}}, A_{\mathrm{LI}}, A_E$	Unit purchase costs of swapper, charger, battery swapping equipment, substation transformer, CBCS transformer, power line, and energy storage.
$A_{\mathrm{BDS},i}, A_{\mathrm{CBCS},j}$	Unit land area prices of BDS *i*, CBCS *j*.
$Y_{\mathrm{CS}}, Y_{\mathrm{E}}$	Service life of charging and swapping network, energy storage.
d	Discount rate.
$N_{\mathrm{BDS}}, N_{\mathrm{CBCS}}, N_S$	Numbers of BDSs, CBCSs, substations.
$O_{\mathrm{SW}}, O_{\mathrm{CH}}, O_{\mathrm{SM}}, O_S, O_{\mathrm{CBCS,T}}, O_{\mathrm{LI}}, O_E$	Annual operation-maintenance unit costs of swapper, charger, battery swapping equipment, substation transformer, CBCS transformer, power line, energy storage.
$R_{D,I}, R_{D,E}$	Coefficients of elimination disposal costs of infrastructure equipment, energy storage.
$P_{\mathrm{Basic}}(t)$	Baseload power.
D	Day numbers per year.
$R_{i,j}, X_{i,j}$	Resistance, reactance of the branch *i,j*.
$P_{L,k,j}(t), Q_{L,k,j}(t)$	Basic load active, reactive powers of node *j*.
$U_{i,\mathrm{MAX}}, U_{i,\mathrm{MIN}}$	Upper, lower limits of node voltage.
$S_{i,j,\mathrm{MAX}}$	Power line *i,j* transmission capacity limit.
$\cos\phi_{\mathrm{T}}$	Power factor
$S_{L,R,k}, S_{T,R,k}$	Substation *k* current baseload, current capacity.
$\chi_T, \chi_S, \delta_{\mathrm{T}}$	Coefficients of redundancy, load simultaneous, rated load rate of transformer.
R_{AR}	Area redundancy coefficient.
$M_B, M_{\mathrm{SW}}, M_C, M_{\mathrm{SM}}$	Unit land areas of battery, swapper, charger, and battery swapping equipment.
$\omega_{\mathrm{CBCS,C},n}, \omega_{\mathrm{BDS,C},m}$	Candidate coordinates of CBCS *n*, BDS *m*.
$A_{\mathrm{CBCS,C},n}, A_{\mathrm{BDS,C},m}$	Unit area costs of candidate coordinates of CBCS *n*, BDS *m*.
A_{BTV}	Unit driving cost of a BTV.

D. VARIABLES

$P_{\mathrm{R},i}(t), P_{\mathrm{C},j}(t), P_{\mathrm{I},k}(t)$	Probabilities of SEV needs swapping battery in residential region *i*, commercial region *j,* and industrial region *k*.
$B_{\mathrm{BDS,f},i}(t)$	Full level battery number of BDS *i*.
$B_{\mathrm{BTV},i}(t)$	Number of full level batteries that are transported by BTV to BDS *i*.
$B_{\mathrm{SEV},i}(t)$	Load number of SEVs in BDS *i*.
$P_{\mathrm{BDS},i}(t), P_{\mathrm{CBCS},j}(t)$	Operating power of BDS *i,* CBCS *j*.
$E_{\mathrm{BDS},i}, E_{\mathrm{CBCS},j}$	Energy storage capacity of BDS *i*, CBCS *j*.
$P_{\mathrm{CBCS,ch},j}(t), P_{\mathrm{CBCS,di},j}(t)$	Charging, discharging powers of CBCS *j*.
$X_{\mathrm{CBCS,ch},j}(t), X_{\mathrm{CBCS,di},j}(t)$	Charging and discharging states of CBCS *j*.
$P_{\mathrm{CBCS,max},j}$	CBCS *j* maximum charging, discharging power.
$N_{\mathrm{CH},j}, N_{\mathrm{SM},j}$	CBCS *j* charger, battery swapping equipment number.
$E_{\mathrm{CBCS,O},j}(t)$	Operating electric quantity of CBCS *j*.
$D_{\mathrm{BTV,sin},i}, D_{\mathrm{BTV,com},i}$	Single, total shortest battery transport distance between BDS *i* to target CBCS.
$(X_{\mathrm{Road},1}, Y_{\mathrm{Road},1})$ $(X_{\mathrm{Road,max}}, Y_{\mathrm{Road,max}})$	First, last road nodes of the BTV driving path.
$D_{\mathrm{BTV},i}(t)$	Total driving distance of BTV from BDS *i* to target CBCS.
$W_{\mathrm{BTV},i}, V_{\mathrm{BTV},i}(t)$	Depart status, speed of BTV.
$F_{1\mathrm{st}}, F_{2\mathrm{st}}$	Upper, lower layer planning objective.
C_I, C_E, C_O, C_D, C_P	Costs of infrastructure, energy storage, operation-maintenance, elimination-disposal, energy purchase of planning.
$L_{\mathrm{CBCS},j}$	Power line length from substation to CBCS j.
$M_{\mathrm{BDS},i}, M_{\mathrm{CBCS},j}$	Land areas of BDS *i*, CBCS *j*.
$P_{i,j}(t), Q_{i,j}(t)$	Active, reactive power of start of branch *i,j*.
$I_{i,j}(t)$	Current flowing through the branch *i,j*.
$P_{\mathrm{CS},cs,u,j}(t), Q_{\mathrm{CS},cs,u,j}(t)$	Active, reactive power of the type *cs* charging and swapping facilities at node *j*
$P_{\mathrm{Loss}}(t), Q_{\mathrm{Loss}}(t)$	Active, reactive powers of network loss.
U_i	Node *i* voltage.
$P_{\mathrm{G},i}(t), Q_{\mathrm{G},i}(t)$	Active, reactive powers of power source.
$\omega_{\mathrm{CBCS},j}, \omega_{\mathrm{BDS},i}$	Planning coordinates of CBCS *j*, BDS *i*.

I. INTRODUCTION

WITH the rapid development of society, the problem of energy shortage and environmental pollution has become apparent increasingly. Electric vehicles (EVs) have the advantages of better energy utilization efficiency, and improved

integration of renewable energy, etc., which is a good choice for the green development of electricity and transportation system. The centralized charging and multipoint distribution mode combines centralized battery charging stations (CBCSs) and battery distribution stations (BDSs) [1]. It can avoid long time charging for EVs, alleviate the random EV load impact on grid, and reduce pollution, etc. The reasonable planning of CBCSs and BDSs considering battery logistics system will not only improve the smooth realization of CBCSs and BDSs projects but also improve the reliability and economy of CBCSs and BDSs construction and operation in the later period. Therefore, it is of great significance to study the scientific and reasonable planning method of CBCSs and BDSs for swapping EVs (SEVs).

At present, most forecasting studies on EVs only focus on charging EVs or electric buses. Qian *et al.* [2] established a model of load demand due to EV battery charging. A spatial and temporal model of charging EV is established in [3]. Hafez and K. Bhattacharya [4] proposed a queuing analysis charging EV load model based on charging behavior. A time-space model for grid impact analysis of charging EV is established in [5]. Yang *et al.* [6] proposed a model for scale evolution demand of charging EV. Chaudhari *et al.* [7] proposed a forecasting method for EV charging load. A charging EVs load forecasting method on the grid is proposed in [8]. Ghiasnezhad Omran and Filizadeh [9] established a forecasting model of EV charging load. In [10], a fast prediction method of EV load in charging stations is proposed. Dai *et al.* [11] established a forecasting model of electric bus battery swap load. A charging EV load forecasting method using the Q-learning is proposed in [12]. A model of electricity demand for charging EVs is established in [13]. Zhang *et al.* [14] proposed a deep-learning forecasting method of EV charging load. However, the above EV forecasting method cannot forecast the time-space load of SEVs [e.g., swapping private EVs (SPEVs) and swapping electric taxis (SETs)]. At present, there are few relevant contents of SEVs forecasting. Therefore, it is important to further study the time-space forecasting method of SEVs, which is the significant basis for optimal planning of the charging and swapping facilities.

A large number of researchers have optimized the planning of EV charging stations. Shaaban *et al.* [15] established a joint planning model of EV charging stations in microgrids. A planning strategy for EV charging stations is proposed in [16]. In [17], a planning method for EV charging stations is proposed. Zeng *et al.* [18] proposed a bilevel planning approach for EV charging stations. An EV fast-charging station siting and sizing planning model is established in [19]. In [20], a planning model for EV charging stations is established. A robust joint expansion planning method for EV charging stations is proposed in [21]. Bayram *et al.* [22] established a capacity planning model for EV charging stations. Some researchers have optimized the planning of EV swapping stations. In [23], a planning approach for EV battery swapping network is proposed. Zheng *et al.* [24] built a planning model of EV battery charging and swapping stations. Wang *et al.* [25] proposed an optimal location method for EV battery swapping stations. A planning model of renewable energy and battery swapping system is established in [26]. Ban *et al.* [27] proposed a sizing planning model for battery swapping stations.

However, most of the existing literatures about CBCS only focused on its dispatching problem, only a few literatures paid attention to its planning problem. An optimization model for charging station, battery swap station, and energy storage system is established in [28]. Gan and Zheng [29] built a planning model of centralized charging stations. Kang *et al.* [30] proposed a charging strategy for battery swapping EVs. In [31], a scheduling method for EV battery charging stations is proposed. A configuration model of EV charging and swapping station is established in [32]. Yongxiang *et al.* [33] investigated a mode of charging stations and battery-swap stations. In [34], an operational planning approach of second-life battery charging stations is proposed. Zhang and Wang [35] built a dispatch model of EV batteries between battery swapping stations and charging stations. In [36], a scheduling method of charging station of battery swapping EVs is proposed. A siting model of EV battery swapping stations with centralized charging is established in [37]. He *et al.* [1] built a planning model for EV CBCS. At present, the researchers including [1] hardly pay attention to the sizing and locating planning of CBCSs and BDSs considering the battery logistics system based on time-space load forecasting of SEVs. This article is the extension of our conference paper [1].

When a charging and swapping facilities planning project is invested by different investors, it is suitable to adopt multi-level planning modeling and solving [38]–[43]. Moradijoz *et al.* [38] present a bilevel model for distribution network planning considering distribution network operators and grid able parking lot owners. A bilevel site and size planning of plug-in EV charging stations is developed in [39]. A bilevel planning strategy for EV fast charging is studied in [40]. A bilevel programming model for planning charging infrastructure in intercity transportation networks is built in [41]. A bilevel planning model of an EV charging station with renewable energy resources is established in [42]. Zeng *et al.* [43] develop a bilevel model, which to optimize the planning of an EV charging station with distributed energy resources. And for solving methods of the double-level programming model, it generally has two ways: double-loop iterative optimization methods are adopted to optimize double-level models [38]–[41]; and A single level programming is transformed from the double-level programming model, then optimized by a single level optimization method [42], [43]. In addition, the earliest and most prominent approaches for solving the shortest path problem are the Bellman–Ford algorithm (BFA), and the BFA presents the fastest known, strictly polynomial algorithm for directed graphs with arbitrary weights [44]. And the well-known and classical BFA guarantees the solution optimality on the shortest path problem [45], [46]. The BFA is the most significant dynamic programming method, and is mostly used to solve problems with a single source vertex [47]. The BFA has more adaptable compared with the Dijkstra algorithm [48]. The BFA is widely used in the optimization problem of vehicle driving paths (see e.g., [44]–[48]).

In this article, a planning method for CBCSs and BDSs considering the battery logistics system is proposed. First, the time-space load forecasting model of SEVs is built. Then,

operation models of CBCS, BDS, and battery logistics system are established. After that, sizing models of CBCSs and BDSs are established. Then, a double-level planning model of CBCSs and BDSs considering battery logistics system is established. Finally, the correctness and effectiveness of the CBCS planning model and method are verified through case studies. The main contributions of this article are summarized as follows.

1) Based on the analysis of characteristics of travel chains of SEVs, including SPEVs and SETs, a time-space load forecasting method for SEVs is proposed. It considers the natures and characteristics of regions in the planning area. It takes into account the driving habits and swapping habits of different types SEV users. And it thinks over the randomness and uncertainty of driving distance, swapping time and site, etc.
2) Operation models of CBCS, BDS, and battery logistics system are established, which are based on detailly service and operation analysis of function and characteristic of CBCS, BDS, and battery logistics system. Afterward, based on the operation models of CBCS and BDS, the sizing models of CBCS and BDS are built.
3) A double-level sizing and locating planning model of CBCSs and BDSs considering the battery logistics system is established. First, the first-level planning takes the planning economy as the goal to optimize the locations and scales of CBCSs and BDSs. Then, considering the annual transport cost of the battery logistics company, second-level planning is established, to minimize the battery logistics system.
4) This article differs from the previous conference paper [1] in the following ways: In the modeling section, the proposed method builds operation models of BDSs and CBCSs, and considers the operation and sizing coupling between BDS, CBCS, and battery logistics system in detail. Moreover, the planning model of CBCS further considers the power purchase cost, and optimizes BDS locations. The SEV load forecasting method more detailed description of SEV time-space distribution characteristics. In the case study section, the following contents are supplemented. First, a new and more representative case study is designed. Second, this article reperforms time-space load forecasting of SEVs for the new case study to show the feasibility and effectiveness of the proposed forecasting method. Third, the impacts of CBCS construction quantities and the way of CBCS participates in grid dispatching on the CBCS and BDS planning and operation are discussed by multi cases. Then, it fully proves the comprehensiveness, effectiveness, and feasibility of the proposed planning method.

The rest of this article is organized as follows. Section II describes the models of centralized charging and multipoint distribution network. Section III establishes the time-space load forecasting model of SEVs. Section IV establishes the operation and sizing models of CBCS, BDS, and the battery logistics system. A double-level planning model of CBCSs and BDSs considering battery logistics system is presented in Section V. Section VI presents the analysis of case studies. Finally, Section VII concludes this article.

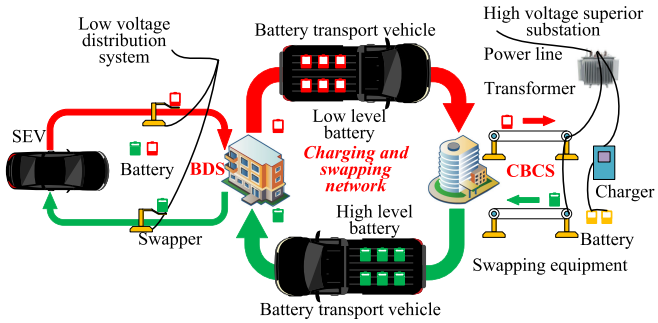

Fig. 1. Centralized charging and multi point distribution network.

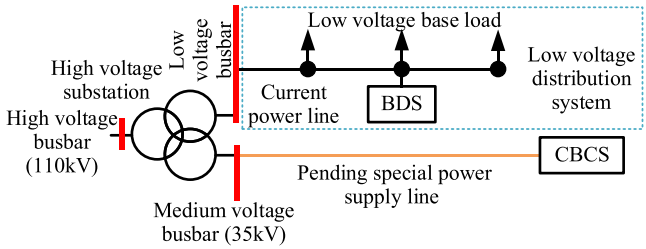

Fig. 2. Distribution systems of CBCSs and BDSs.

II. Centralized Charging and Multipoint Distribution Network

The centralized charging and multipoint distribution network are one of the main ways in SEVs energy supply. The main characteristics of this network are as follows.

1) SEVs put on the high-level batteries in BDSs, and put off the low-level batteries in BDSs. In addition, BDSs do not have the charging function, but only serve as places for EV users to obtain battery swapping services.
2) The battery logistics system is responsible for transporting low-level batteries from BDSs to CBCSs. Then, it transports high-level batteries from CBCS to BDSs for EVs swapping. The batteries transportation is supplied by battery logistics companies.
3) CBCSs centrally charge a large quantity of batteries.

The centralized charging and multipoint distribution network are shown in Fig. 1. The distribution systems of CBCSs and BDSs are shown in Fig. 2. It has the following advantages.

1) Energy supplement durations of SEVs are short.
2) Utilizations of chargers and swappers are high.
3) A friendlier charging scheme is formulated easily for the grid.

III. Time-Space Load Forecasting of SEVs

The load uncertainty of SEVs increases the planning difficulty of the CBCSs. Therefore, SPEVs and SETs in the planning area are analyzed for their forecasting. Their travel chains are shown in Fig. 3. Multiscenario sampling technology can effectively solve the problem of randomness [49]. Scenarios are forecasted for the SEV time-space load model in this article. The K-means clustering method is adopted to reduce the scenarios [50].

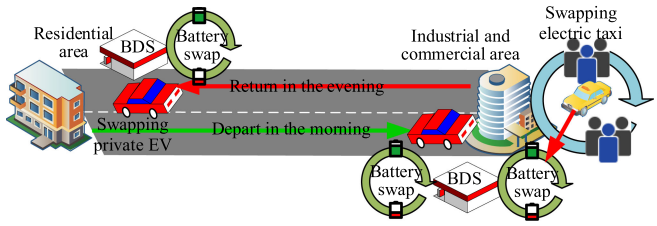

Fig. 3. Travel chains of SPEVs and SETs.

A. Travel Chain Analysis of SPEVs

Except for the difference in the energy supplying forms (i.e., charging and swapping), the vehicle parameters (i.e., EV capacity, etc.) of SEVs are the same as that of charging EVs. Moreover, users' driving habits are similar to SEVs and charging EVs. Undoubtedly, the battery swapping time of a SEV and the initial charging time of a charging EV can be regarded as the same. That is, the distribution function of swapping time t_0 can be written as (1) [51]. And the SPEV daily driving distance l satisfies the probability distribution of (2) [51]

$$f_S(t_0)=\begin{cases}\frac{1}{\sigma_S\sqrt{2\pi}}\exp\left[-\frac{(t_0-\mu_S)^2}{2\sigma_S^2}\right], \mu_S-12<t_0\le 24\\ \frac{1}{\sigma_S\sqrt{2\pi}}\exp\left[-\frac{(t_0+24-\mu_S)^2}{2\sigma_S^2}\right], 0<t_0\le \mu_S-12\end{cases} \tag{1}$$

where $\mu_{\rm S}$ and $\sigma_{\rm S}$ are the parameters of the initial charging time distribution of a charging EV, and $\mu_S=17.6$, $\sigma_S=3.4$.

$$f_D(l)=\frac{1}{l\sigma_D\sqrt{2\pi}}\exp\left[-\frac{(\ln l-\mu_D)^2}{2\sigma_D^2}\right] \tag{2}$$

where $\mu_{\rm D}=3.2$ and $\sigma_{\rm D}=0.88$.

Generally, an SPEV user drives from a residential region to an industrial region or commercial region in the morning, and returns to the residential region in the evening. As a result, in the morning (5:00–18:00), the SPEVs concentrate in industrial/commercial areas generally. In the evening (0:00–5:00 and 18:00–24:00), the SPEVs gather in residential areas commonly. In addition, different types of areas (i.e., residential area, industrial area, and commercial area) in the planning area are numbered. After that, the area numbers of SPEVs swap batteries are sampled.

The swapping probability of SPEV in residential region is equal to the ratio of the region population to the planning area's total population. The swapping probability of SPEV in industrial/commercial regions are equal to the ratio of region areas to the total planning area. The time-space distribution probability of SPEVs satisfies

$$\begin{cases}\sum P_{R,i}(t):\sum P_{C,j}(t):\sum P_{I,k}(t)=7:2:1,\\ \quad t\in[0,5]\cup[18,24]\\ \sum P_{R,i}(t):\sum P_{C,j}(t):\sum P_{I,k}(t)=3:4:3,\quad \forall i,j,k\\ \quad t\in[5,18]\\ \sum P_{R,i}(t)+\sum P_{C,j}(t)+\sum P_{I,k}(t)=1\ \forall t\end{cases} \tag{3}$$

$$\begin{cases}P_{R,n}(t)/\sum P_{R,i}(t)=N_{{\rm RP},n}/N_{\rm RP,Total}\\ P_{C,n}(t)/\sum P_{C,j}(t)=M_{C,n}/M_{C,\rm Total}\\ P_{I,n}(t)/\sum P_{I,k}(t)=M_{I,n}/M_{I,\rm Total}\end{cases}\quad \forall t,i,j,k \tag{4}$$

where $P_{R,i}(t)$, $P_{C,j}(t)$, and $P_{I,k}(t)$ are the probabilities of SEV needs swapping battery in residential region i, commercial region j, and industrial region k at time t, respectively. $N_{{\rm RP},n}$ and $N_{\rm RP,Total}$ are the population of residential region n and whole planning area respectively. $M_{C,n}$ and $M_{C,\rm Total}$ are the area of commercial region n and total commercial region area respectively. $M_{I,n}$ and $M_{I,\rm Total}$ are the area of industrial area n and total industrial region area respectively.

B. Travel Chain Analysis of SETs

SETs are commercial vehicles and generally work in a state of long-distance driving. The average daily mileage of taxis is 350–500 km. Thus, an SET swaps battery twice on a daily basis generally. Simultaneously, taxi drivers do not have rest during the operating period commonly. Therefore, they generally select to swap batteries at shift handover, lunch, and dinner. The time-space distribution probability of SETs satisfies

$$\begin{cases}\sum P_{R,i}(t):\sum P_{C,j}(t):\sum P_{I,k}(t)\\ \quad =7:2:1, t\in[5,8]\\ \sum P_{R,i}(t):\sum P_{C,j}(t):\sum P_{I,k}(t)\\ \quad =1:2:2, t\in[11,13]\\ \sum P_{R,i}(t):\sum P_{C,j}(t):\sum P_{I,k}(t)\\ \quad =2:1:1, t\in[18,20]\\ \sum P_{R,i}(t):\sum P_{C,j}(t):\sum P_{I,k}(t)\\ \quad =1:1:1, t\in \text{Other time}\\ \sum P_{R,i}(t)+\sum P_{C,j}(t)+\sum P_{I,k}(t)=1\ \forall t\end{cases}\quad \forall i,j,k \tag{5}$$

$$\begin{cases}P_{R,n}(t)/\sum P_{R,i}(t)=M_{R,n}/M_{P,\rm Total}\\ P_{C,n}(t)/\sum P_{C,j}(t)=M_{C,n}/M_{C,\rm Total}\\ P_{I,n}(t)/\sum P_{I,k}(t)=M_{I,n}/M_{I,\rm Total}\end{cases}\quad \forall t,i,j,k \tag{6}$$

where $M_{R,n}$ and $M_{R,\rm Total}$ are the area of residential region n and total residential region area, respectively.

IV. Sizing and Operation Model of the Centralized Charging and Multipoint Distribution Network

With detailed analysis based on the functions and characteristics of the BDS, CBCS, and battery in the transportation system, the operation models of BDS, CBCS, and battery transport system are built. Then, sizing models of BDS and CBCS are established.

A. Sizing and Operation Models of BDS

1) Operation Model of BDS: The operation model of BDS is established, which satisfies (7). In other words, the full level battery number of BDS, number of full level batteries transported by battery transport vehicles (BTVs), and SEVs number of BDS satisfy the following time coupling relationship

$$\begin{cases}B_{{\rm BDS},f,i}(t)=B_{{\rm BDS},f,i}(t-1)+B_{{\rm BTV},i}(t-1)\\ \quad -B_{{\rm SEV},i}(t-1)\\ P_{{\rm BDS},i}(t)=P_{{\rm SW},N}\,\text{ceil}\left\{\frac{B_{{\rm SEV},i}(t)}{N_{{\rm SW},N}}\right\}\end{cases}\quad \forall t \tag{7}$$

where $B_{\mathrm{BDS},f,i}(t)$ is the full level battery number of BDS *i* at time *t*. $B_{\mathrm{BTV},i}(t)$ is the number of full-level batteries that are transported by BTV to BDS *i* at time *t*. $B_{\mathrm{SEV},i}(t)$ is the load number of SEVs in BDS *i* at time *t*. $N_{\mathrm{SW},N}$ is the rated number of SEVs that can be serviced by one swapper in a unit of time. $P_{\mathrm{BDS},i}(t)$ is the operating power of BDS *i* at time *t*. $P_{\mathrm{SW},N}$ is the rated power of the swapper.

2) Sizing Model of BDS: The main types of equipment for BDS are SEV battery energy storage, and battery swappers. The capacity of SEV energy storage and the number of swappers meet the SEV load demand at each time, which satisfies

$$\begin{cases} E_{\mathrm{SEV}}\mathrm{ceil}\left\{(1+\eta_{\mathrm{BDS}})B_{\mathrm{BDS},f,i}(t)\right\} \le E_{\mathrm{BDS},i} \\ \mathrm{ceil}\left\{(1+\eta_{\mathrm{SW}})\frac{B_{\mathrm{SEV},i}(t)}{N_{\mathrm{SW},n}}\right\} \le N_{\mathrm{SW},i} \end{cases} \forall t \quad (8)$$

where E_{SEV} is the SEV energy storage capacity. η_{BDS} is the capacity redundancy coefficient of BDS energy storage. $E_{\mathrm{BDS},i}$ is the energy storage capacity of BDS *i*. η_{SW} is the swapper redundancy coefficient.

B. Planning and Operation Models of CBCS

1) Operation Model of CBCS: The operation model of CBCS shows in

$$\begin{cases} P_{\mathrm{CBCS},j}(t) = P_{\mathrm{CBCS,ch},j}(t)\eta_{\mathrm{CH}} - \frac{P_{\mathrm{CBCS},di,j}(t)}{\eta_{\mathrm{DI}}} \\ 0 \le P_{\mathrm{CBCS,ch},j}(t) \le P_{\mathrm{CBCS,max},j}X_{\mathrm{CBCS,ch},j}(t) \\ 0 \le P_{\mathrm{CBCS},di,j}(t) \le P_{\mathrm{CBCS,max},j}X_{\mathrm{CBCS,di},j}(t) \\ X_{\mathrm{CBCS,ch},j}(t) + X_{\mathrm{CBCS},di,j}(t) \le 1 \\ P_{\mathrm{CBCS,max},j} = N_{\mathrm{CH},j}P_{\mathrm{CH},N} \\ E_{\mathrm{CBCS},O,j}(t) = E_{\mathrm{CBCS,O},j}(t-1) + \\ P_{\mathrm{CBCS},j}(t-1)\Delta T - \sum_{i\in\mathrm{CBCS}(j)} B_{\mathrm{BTV},i}(t-1) \\ \mathrm{SOC_{MIN}}E_{\mathrm{CBCS},j} \le E_{\mathrm{CBCS,O},j}(t) \le \mathrm{SOC_{MAX}}E_{\mathrm{CBCS},j} \end{cases} \forall t \quad (9)$$

where $P_{\mathrm{CBCS},j}(t)$ is the operating power of CBCS *j* at time *t*. $P_{\mathrm{CBCS,ch},j}(t)$ and $P_{\mathrm{CBCS,di},j}(t)$ are the charging and discharging powers of CBCS *j* at time *t,* respectively. η_{CH} and η_{DI} are the charging and discharging efficiency of energy storage, respectively. $X_{\mathrm{CBCS,ch},j}(t)$ and $X_{\mathrm{CBCS,di},j}(t)$ are the charging and discharging states of CBCS *j* at time *t* respectively. $P_{\mathrm{CBCS,max},j}$ is the maximum value of charging and discharging power of CBCS *j*. $N_{\mathrm{CH},j}$ is the charger number of CBCS *j*. $P_{\mathrm{CH},N}$ is the rated power of the charger. $E_{\mathrm{CBCS,O},j}(t)$ is the operating electric quantity of CBCS *j* at time *t*. ΔT is the unit time slot, which is equal to 1h. $\mathbf{CBCS}(j)$ is the set of BDSs that is the energy supplied by CBCS *j*. $E_{\mathrm{CBCS},j}$ is the energy storage capacity of CBCS *j*. $\mathrm{SOC_{MAX}}$ and $\mathrm{SOC_{MIN}}$ are the upper and lower limits of energy storage, respectively.

2) Sizing Model of CBCS: The main types of equipment of CBCS are chargers, swapping equipment, and SEV battery energy storage. The SEV battery energy storage capacities, swapper numbers, and charger numbers meet the SEV battery demand of the BTVs at each time, which satisfies

$$\begin{cases} E_{\mathrm{SEV}}\mathrm{ceil}\left\{\frac{(1+\eta_{\mathrm{CBCS}})E_{\mathrm{CBCS},O,j}(t)}{\mathrm{SOC_{max}}E_{\mathrm{SEV}}}\right\} \le E_{\mathrm{CBCS},j} \\ \mathrm{ceil}\left\{(1+\eta_{\mathrm{CHA}})\frac{E_{\mathrm{CBCS},j}}{E_{\mathrm{EV}}N_{\mathrm{CH,N}}}\right\} \le N_{\mathrm{CH},j} \\ \mathrm{ceil}\left\{(1+\eta_{\mathrm{SM}})\frac{\sum_{i\in\mathrm{CBCS}(j)}B_{\mathrm{BTV},i}(t)}{N_{\mathrm{SM},N}}\right\} \le N_{\mathrm{SM},j} \end{cases} \forall t \quad (10)$$

where η_{CBCS} is the capacity redundancy coefficient of CBCS energy storage. η_{CHA} is the redundancy coefficient of the charger. $N_{\mathrm{CH},N}$ is the rated number of batteries that can be charged by one charger simultaneously. η_{SM} is the redundancy coefficient of battery swapping equipment in CBCS. $N_{\mathrm{SM},j}$ is the number of battery swapping equipment of CBCS *j*.

C. Battery Logistics System Model

To reduce the battery transport cost of the battery logistics company, BTVs choose the shortest driving route commonly. And the shortest battery transport distance between BDS *i* and CBCS *j* satisfies

$$\begin{cases} D_{\mathrm{BTV,sin},i} = \sum_{n,m\in\boldsymbol{R}(i,j)} |(X_{\mathrm{Road},n}, Y_{\mathrm{Road},n}), \\ \quad (X_{\mathrm{Road},m}, Y_{\mathrm{Road},m})|_2 \\ (X_{\mathrm{BDS},i}, Y_{\mathrm{BDS},i}) = (X_{\mathrm{Road},1}, Y_{\mathrm{Road},1}) \\ (X_{\mathrm{CSCS},j}, Y_{\mathrm{CSCS},j}) = (X_{\mathrm{Road,max}}, Y_{\mathrm{Road,max}}) \end{cases} \quad (11)$$

where $D_{\mathrm{BTV,sin},i}$ is the single shortest battery transport distance from BDS *i* to target CBCS. $(X_{\mathrm{Road},n}, Y_{\mathrm{Road},n})$ is the road node *n*. $(X_{\mathrm{Road},1}, Y_{\mathrm{Road},1})$ is the first road node of the driving path of the BTV (that is, the road node corresponding to the departure BDS). $(X_{\mathrm{Road,max}}, Y_{\mathrm{Road,max}})$ is the last road node of the driving path of the BTV (that is, the road node corresponding to the target CBCS). $\boldsymbol{R}(i,j)$ is the road node set of BTV driving path.

First, the BTV departs from its BDS to the nearest CBCS. Second, it comes back to the BDS. So, it is clear that the total transport distance needs to be calculated twice, which meets

$$D_{\mathrm{BTV,com},i} = N_{\mathrm{BTV,CI}}D_{\mathrm{BTV,sin},i} \quad (12)$$

where $D_{\mathrm{BTV,com},i}$ is the total driving distance of a BTV that completes a battery transport task. $N_{\mathrm{BTV,CI}}$ is the round trip times of a BTV that completes a battery transport task.

Only a BDS has low-level batteries, the BTVs will drive to CBCS for exchanging high-level batteries. The departure constraint of battery logistics vehicles satisfies (13) and (14). And the logistics driving duration satisfies (15)

$$D_{\mathrm{BTV},i}(t) = W_{\mathrm{BTV},i}(t)D_{\mathrm{BTV,com},i} \quad (13)$$

$$\begin{cases} W_{\mathrm{BTV},i}(t) = 1, B_{\mathrm{BDS,f},i}(t) \le B_{\mathrm{BDS,f,max},i} \\ W_{\mathrm{BTV},i}(t) = 0, B_{\mathrm{BDS,f},i}(t) = B_{\mathrm{BDS,f,max},i} \end{cases} \quad (14)$$

$$\frac{D_{\mathrm{BTV},i}(t)}{V_{\mathrm{BTV},i}(t)} \le T_{\mathrm{BTV,MAX}} \ \forall i \ \forall t \quad (15)$$

where $D_{\mathrm{BTV},i}(t)$ is the driving distance of the BTV from BDS *i* to target CBCS at time *t*. The binary constant $W_{\mathrm{BTV},i}$ represent the status of BTV, i.e., 1 represents that EV departs, 0 represents that EV doesn't depart. $V_{\mathrm{BTV},i}(t)$ is the speed of BTV at time *t*, and $V_{\mathrm{BTV},i}(t) \sim N$[5], [25]. $T_{\mathrm{BTV,MAX}}$ is the maximum transportation duration.

V. Double-Level Planning Model of CBCSS Considering Battery Transport System

The double-level planning model of CBCSs and BDSs is established in this article. Above all, the upper layer optimization goal is the life cycle cost (LCC) of the planning. Moreover, the

lower layer planning objective is the annual transportation cost of the battery logistics company.

A. The Upper Layer Planning

The upper layer planning considers the planning LCC of charging and swapping facilities (i.e., CBCS and BDS), substation expansion, and power line, etc., which is regarded as the goal.

1) Objective: The objective (planning LCC) of the upper layer planning F_{1st} is defined as follows:

$$\min F_{1\text{st}} = C_I + C_E + C_O + C_D + C_P \tag{16}$$

where C_I, C_E, C_O, C_D, and C_P are the costs of infrastructure, energy storage, operation maintenance, elimination-disposal, and energy purchase of planning, respectively. Each section cost in the above objective function satisfies (17)–(21).

a) Infrastructure cost: The infrastructure cost of the planning includes the costs of chargers, swappers, transformers, swapping equipment, area, and power lines of BDSs and CBCSs, as well as the capacity expansion of substations, which satisfies

$$\begin{aligned} C_I = \frac{d(1+d)^{Y_{\text{CS}}}}{(1+d)^{Y_{\text{CS}}}-1}\Bigg[&\sum_{i=1}^{N_{\text{BDS}}}\left(A_{\text{SW}}N_{\text{SW},i}+A_{\text{BDS},i}M_{\text{BDS},i}\right) \\ &+\sum_{k=1}^{N_{\text{S}}}A_{\text{S}}S_{S,k}+\sum_{j=1}^{N_{\text{CBCS}}}\Big(A_{\text{CH}}N_{\text{CH},j}+A_{\text{SM}}N_{\text{SM},j} \\ &+A_{\text{CBCS},j}M_{\text{CBCS},j} \\ &+A_{\text{CBCS,T}}S_{\text{CBCS},T,j}+A_{\text{LI}}L_{\text{CBCS},j}\Big)\Bigg] \end{aligned} \tag{17}$$

where A_{SW}, A_{CH}, and A_{SM} are the purchase costs of swapper, charger, and battery swapping equipment, respectively. A_{S} and $A_{\text{CBCS,T}}$ are the purchase costs of unit transformer capacities of substation and CBCS respectively. A_{LI} is the unit of length price of a power line. $L_{\text{CBCS},j}$ is the pending power line length from the substation to CBCS *j*. $M_{\text{BDS},i}$ and $M_{\text{CBCS},j}$ are the land areas of BDS *i* and CBCS *j*, respectively. $A_{\text{BDS},i}$ and $A_{\text{CBCS},j}$ are the unit land area prices of BDS *i* and CBCS *j*, respectively. Y_{CS} is the service life of charging and swapping network. d is the discount rate. N_{BDS}, N_{CBCS}, and N_S are the numbers of BDSs, CBCSs, and substations, respectively.

b) Energy storage cost: The energy storage cost mainly includes the energy storage acquisition cost of BDS and CBCS

$$C_E=\frac{A_E d(1+d)^{Y_E}}{(1+d)^{Y_E}-1}\left(\sum_{i=1}^{N_{\text{BDS}}}E_{\text{BDS},i}+\sum_{j=1}^{N_{\text{CBCS}}}E_{\text{CBCS},j}\right) \tag{18}$$

where A_E is the unit capacity price of energy storage. Y_E is the service life of energy storage.

c) Operation-maintenance cost:

$$\begin{aligned} C_O = &\sum_{i=1}^{N_{\text{BDS}}}O_{\text{SW}}N_{\text{SW},i}+\sum_{k=1}^{N_{\text{S}}}\left(O_S S_{S,k}\right)+\sum_{j=1}^{N_{\text{CBCS}}}\left(O_{\text{CH}}N_{\text{CH},j}\right. \\ &\left.+O_{\text{SM}}N_{\text{SM},j}+O_{\text{CBCS},T}S_{\text{CBCS},T,j}+O_{\text{LI}}L_{\text{CBCS},j}\right) \\ &+O_E\left(\sum_{i=1}^{N_{\text{BDS}}}E_{\text{BDS},i}+\sum_{j=1}^{N_{\text{CBCS}}}E_{\text{CBCS},j}\right) \end{aligned} \tag{19}$$

where O_{SW}, O_{CH}, and O_{SM} are the annual operation-maintenance costs of swapper, charger, and battery swapping equipment, respectively. O_S and $O_{\text{CBCS},T}$ are the annual operation-maintenance costs of unit transformer capacities of substation and CBCS respectively. O_{LI} is the annual operation-maintenance cost of unit length power line. O_E is the annual operation-maintenance cost of energy storage unit capacity.

d) Elimination-disposal cost: The elimination-disposal cost is brought by the charging and swapping equipment, energy storage, transformer, power line, etc.,

$$\begin{aligned} C_D = &\frac{R_{D,I}d}{(1+d)^{Y_{\text{CS}}}-1}\Bigg[\sum_{i=1}^{N_{\text{BDS}}}\left(A_{\text{SW}}N_{\text{SW},i}\right) \\ &+\sum_{k=1}^{N_S}\left(A_S S_{S,k}\right)+\sum_{j=1}^{N_{\text{CBCS}}}\Big(A_{\text{CH}}N_{\text{CH},j} \\ &+A_{\text{SM}}N_{\text{SM},j}+A_{\text{CBCS},T}S_{\text{CBCS},T,j}+A_{\text{LI}}L_{\text{CBCS},j}\Big)\Bigg] \\ &+\frac{R_{D,E}A_E d}{(1+d)^{Y_E}-1}\left(\sum_{i=1}^{N_{\text{BDS}}}E_{\text{BDS},i}+\sum_{j=1}^{N_{\text{CBCS}}}E_{\text{CBCS},j}\right) \end{aligned} \tag{20}$$

where $R_{D,I}$ and $R_{D,E}$ are the coefficients of elimination disposal costs of infrastructure equipment and energy storage equipment, respectively.

e) Energy purchase cost: Energy purchase cost includes the purchase costs of basic load and CBCS load

$$C_P=\Delta T D\sum_{t=1}^{T}\left[P_{\text{Basic}}(t)+\sum_{j=1}^{N_{\text{CBCS}}}P_{\text{CBCS},j}(t)\right] \tag{21}$$

where $P_{\text{Basic}}(t)$ is the baseload power at time *t*. T are the time numbers per day. D are the day numbers per year.

2) Constraints: The planning of charging and swapping facilities must meet the constraints of power flow, grid security, transformer capacity, and station building, which are as follows.

a) Power Flow Constraints: The grid power flow is described by Dist-Flow power flow, which satisfies (22). And the network power loss satisfies (23)

$$\begin{cases} \sum_{m\in\Omega(j)}P_{j,m}(t)=P_{i,j}(t)-R_{i,j}|I_{i,j}(t)|^2-P_j(t) \\ \sum_{m\in\Omega(j)}Q_{j,m}(t)=Q_{i,j}(t)-X_{i,j}|I_{i,j}(t)|^2-Q_j(t) \\ P_j(t)=\sum_{\forall u}P_{\text{CS},cs,u,j}(t)+\sum_{\forall k}P_{L,k,j}(t) \\ Q_j(t)=\sum_{\forall u}Q_{\text{CS},cs,u,j}(t)+\sum_{\forall k}Q_{L,k,j}(t) \\ |U_j(t)|^2=|U_i(t)|^2-2(P_{i,j}(t)R_{i,j}+Q_{i,j}(t)X_{i,j}) \\ +(R_{i,j}^2+X_{i,j}^2)|I_{i,j}(t)|^2 \\ |I_{i,j}(t)|^2=\left[P_{i,j}^2(t)+Q_{i,j}^2(t)\right]\Big/|U_{i,j}|^2 \end{cases}, cs\in\text{CS} \tag{22}$$

$$P_{\text{Loss}}(t)=\sum_{i,j\in \boldsymbol{N}_{\text{Grid}}}\left(R_{i,j}|I_{i,j}(t)|^2\right) \tag{23}$$

where, $\boldsymbol{\Omega}(j)$ is the set of the end nodes which belong to the branch with the same start node *j*. $P_{i,j}(t)$ and $Q_{i,j}(t)$ are the active and reactive power of the start of branch *i,j* at time *t,* respectively. $I_{i,j}(t)$ is the current flowing through the branch *i,j* at time *t*. $R_{i,j}$and $X_{i,j}$are the resistance and reactance of the branch *i,j* , respectively. $P_{\text{CS},cs,u,j}(t)$ and $Q_{\text{CS},cs,u,j}(t)$ are the active and reactive power of the type cs charging and swapping facilities at node *j* at time *t,* respectively. $P_{L,k,j}(t)$ and $Q_{L,k,j}(t)$are the active and reactive power of the basic load at node *j* at time *t* respectively. $P_{\text{Loss}}(t)$ is the active power loss of the network. $\boldsymbol{N}_{\text{Grid}}$ is the grid node set.U_i is the voltage of node *i*. $\boldsymbol{CS}$ is the type set of charging and swapping facilities.

b) Grid security constraints: The power balance constraint satisfies (24). And the voltage upper limit constraint and the power line transmission constraint satisfy (25) and (26), respectively,

$$\begin{cases}\sum_{\forall i}P_{\text{G},i}(t)-\sum_{\forall u}P_{\text{CS},cs,u}(t)\\ \quad-\sum_{\forall k}P_{\text{L},k}(t)-P_{\text{Loss}}(t)=0\\ \sum_{\forall i}Q_{\text{G},i}(t)\sum_{\forall u}Q_{\text{CS},cs,u}(t)\\ \quad-\sum_{\forall k}Q_{\text{L},k}(t)-Q_{\text{Loss}}(t)=0\end{cases},cs\in\text{CS} \tag{24}$$

$$U_{i,\text{MIN}}\le U_i(t)\le U_{i,\text{MAX}} \tag{25}$$

$$P_{i,j}^2(t)+Q_{i,j}^2(t)\le S_{i,j,\text{MAX}}^2 \tag{26}$$

where $Q_{\text{Loss}}(t)$ is the reactive power loss of the network. $P_{G,i}(t)$ and $Q_{G,i}(t)$ are the active and reactive powers of the power source at time *t,* respectively. $U_{i,\text{MAX}}$ and $U_{i,\text{MIN}}$are the upper and lower limits of node voltage respectively. $S_{i,j,\text{MAX}}$is the transmission capacity upper limit of the power line *i,j*.

c)Transformer capacity constraint:

$$\begin{cases}\dfrac{\max\left\{\sum_{j\in\text{Tra}(k)}P_{\text{CBCS},j}(t)\Big/\cos\phi_T+S_{L,R,k}-\delta_{\text{T}}S_{T,R,k},0\right\}}{\delta_T}\\ \quad\le S_{S,k}\\ \dfrac{(1+\chi_T)\chi_S(N_{\text{CH},j}P_{\text{CH},N}+N_{\text{SM},j}P_{\text{SM},N})}{\delta_T\cos\phi_T}\le S_{\text{CBCS},j,T}\end{cases}\forall t,k,j \tag{27}$$

$$S_{\text{S},k},S_{\text{CBCS},j,T}\in\boldsymbol{S}_{T,n}\ \forall k\ \forall j \tag{28}$$

where $\mathbf{Tra}(k)$ is the set of CBCSs supplied by the substation *k*. $\cos\phi_T$ is the power factor. $S_{L,R,k}$ and $S_{T,R,k}$are the current baseload and current capacity of substation *k,* respectively. χ_T and χ_S are the redundancy coefficient and load simultaneous coefficient respectively. $P_{\text{SM},N}$ is the rated power of swapping equipment. δ_T is the rated load rate. $\boldsymbol{S}_{T,n}$ is the set of rated transformer capacity.

d) Station building constraints: The station areas and planning locations of CBCSs and BDSs meet (29) and (30), respectively. The area unit price at candidate sites meets (31)

$$\begin{cases}(1+\eta_{\text{AR}})\left(M_BE_{\text{CBCS},j}+M_CN_{\text{CH},j}+M_{\text{SM}}N_{\text{SM},j}\right)\\ \quad\le M_{\text{CBCS},j}\\ (1+\eta_{\text{AR}})\left(M_BE_{\text{BDS},i}+M_{\text{SW}}N_{\text{SW},i}\right)\le M_{\text{BDS},i}\end{cases}\forall i,j \tag{29}$$

$$\begin{cases}\omega_{\text{CBCS},j}=(X_{\text{CBCS},j},Y_{\text{CBCS},j})\in\boldsymbol{Z}_{\text{CBCS}}\\ \omega_{\text{BDS},i}=(X_{\text{BDS},i},Y_{\text{BDS},i})\in\boldsymbol{Z}_{\text{BDS}}\end{cases}\forall i,j \tag{30}$$

$$\begin{cases}A_{\text{CBCS},j}=A_{\text{CBCS},C,n},\omega_{\text{CBCS},j}\\ \quad=\omega_{\text{CBCS},C,n}\in\boldsymbol{Z}_{\text{CBCS}}\\ A_{\text{BDS},i}=A_{\text{BDS},C,m},\omega_{\text{BDS},i}\\ \quad=\omega_{\text{BDS},C,m}\in\boldsymbol{Z}_{\text{BDS}}\end{cases}\forall i,j,n,m \tag{31}$$

where R_{AR} is the redundancy coefficient of area. M_B, M_{SW}, M_C , $M_{\text{SM}}$are the land areas of unit capacity battery, swapper, charger, and swapping equipment respectively. $\omega_{\text{CBCS},j}=(X_{\text{CBCS},j}\,,Y_{\text{CBCS},j})$ and $\omega_{\text{BDS},i}=(X_{\text{BDS},i}\,,Y_{\text{BDS},i})$ are the planning coordinates of CBCS *j* and BDS *i*, respectively. $\boldsymbol{Z}_{\text{CBCS}}$ and $\boldsymbol{Z}_{\text{BDS}}$ are the location set of CBCS and BDS, respectively. $\omega_{\text{CBCS,C},n}=(X_{\text{CBCS,C},n},Y_{\text{CBCS,C},n})$ and $\omega_{\text{BDS,C},m}=(X_{\text{BDS,C},m},Y_{\text{BDS,C},m})$ are the candidate coordinates of CBCS *n* and BDS *m*, respectively. $A_{\text{CBCS,C},n}$and $A_{\text{BDS,C},m}$ are the unit area costs of candidate coordinates of CBCS *n* and BDS *m*, respectively.

B. Lower Layer Planning

The lower layer planning objective is the annual transportation cost of the battery logistics company

$$\min F_{2\text{st}}=A_{\text{BTV}}D\sum_{\forall i}\sum_{\forall t}D_{\text{BTV},i}(t) \tag{32}$$

where A_{BTV} is the unit driving cost of a BTV.

C. Model Solution

In many researches on the planning of EV charging and swapping facilities, double-level planning models are built, which are optimized by double-loop iterative optimization methods (see e.g., [38]–[41]). Then, the optimization planning results obtained from the above researches are well, which verified the feasibility, effectiveness, and superiority of modeling and double-loop solving of double-level planning [38]–[41].

Essentially, the planning models of upper and lower layers are a nonconvex nonlinear programming problem (i.e., to minimize cost, Yuan) and a shortest path optimization problem (i.e., to minimize the transport distance of BTVs, km) in this article, respectively. Furthermore, the investment stakeholders of the upper and lower layers in this article are different, which are grid and battery logistics company, respectively. The locations and sizes planning of CBCSs and BDSs will greatly affect the transport distance of BTVs, which greatly affects the economy of battery logistics company. On the other hand, the transportation process of BTVs will greatly affect the reliability of the battery swapping service of the whole charging and swapping network. Therefore, in aspects of planning configuration and operation, there are close coupling coordination relationships between both above. Thus, that is very suitable to use double-level planning for optimization modeling and solving. And such double-level problems cannot be simply solved by the conventional optimization techniques [38]. Therefore, a double-loop iterative optimization method is developed to solve the double-level planning model built in this article. Certainly, the models and solving methods at different layers are not independent in this article, but constitute a

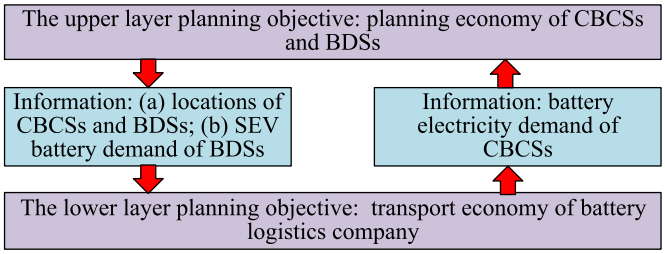

Fig. 4. Model solving process.

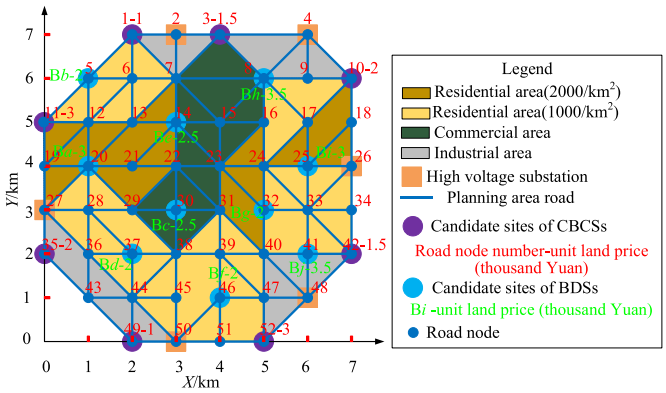

Fig. 5. Planning area.

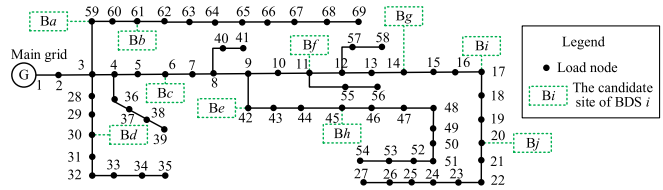

Fig. 6. Network of PG&E69 system.

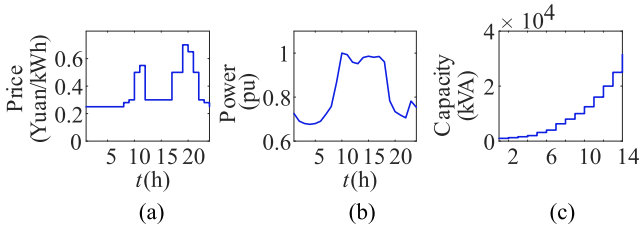

Fig. 7. Basic parameters. (a) Unit electricity purchase price. (b) Basic load power. (c) Transformer rated capacities.

complementary circular comprehensive optimization method of collaborative optimization. That is, the collaborative optimization solutions of each layer objective are realized through the optimization information transmission and interaction between the different layers.

Besides, the BFA is a classic shortest path optimization algorithm, and is widely used in aspects of the vehicle driving path optimization (see e.g., [44]–[48]), which guarantees the solution optimality on the shortest path problem [45], [46]. Therefore, the BFA is used to optimize the BTVs' transport path in the lower layer planning in this article.

The CPLEX toolbox and the Bellman-Ford algorithm are used to solve the planning model above established. The BFA is used to solve the shortest path problem [44]–[48] (e.g., battery logistics path, and power line path of CBCSs). The optimization model proposed in this article is a large-scale, nonconvex, nonlinear combinatorial optimization problem, which is difficult to be solved directly. For the nonconvex nonlinear power flow, the convex relaxation method is used to transform it into a second-order cone programming problem. Then, the proposed model can be transformed into a second-order cone optimization model that can be efficiently solved by a widely used commercial CPLEX toolbox. The model solving process in this article is shown in Fig. 4.

VI. Case Study

A. Parameter Setting

The test example for CBCSs planning area is shown in Fig. 5. The related parameters of planning are shown in Figs. 6 and 7,

TABLE I
Parameters

Parameter	Value	Parameter	Value
$P_{\mathrm{SW,N}}$(kW)	5	A_{E}(k Yuan/kWh)	0.6
E_{SEV}(kWh)	50	Y_{E}(Year)	10
η_{BDS}	1	O_{SW}(k Yuan/year)	0.1
η_{SW}	0.4	O_{CH}(k Yuan/year)	0.5
$N_{\mathrm{SW,N}}$	4	O_{SM}(k Yuan/year)	0.1
$\eta_{\mathrm{CH}}/\eta_{\mathrm{DI}}$	0.9/0.9	O_{S}(k Yuan/(kVA · year))	0.03
$P_{\mathrm{CH,N}}$(kW)	250	$O_{\mathrm{CBCS,T}}$(k Yuan/(kVA · year))	0.01
$SOC_{\mathrm{MAX}}/SOC_{\mathrm{MIN}}$	0.95/0.2	O_{LI}(k Yuan/(m · year))	1
η_{CBCS}	0.5	O_{E}(k Yuan/(kWh · year))	0.05
η_{CHA}	0.2	$R_{\mathrm{D,I}}$	0.1
$N_{\mathrm{CH,N}}$	5	$R_{\mathrm{D,E}}$	0.2
η_{SM}	0.2	T	24
$N_{\mathrm{BTV,CI}}$	2	D	356
$T_{\mathrm{BTV,MAX}}$(h)	1	$U_{i,\mathrm{MAX}}$	1.1pu
A_{SW}(k Yuan)	250	$U_{i,\mathrm{MIN}}$	0.9pu
A_{CH}(k Yuan)	100	$cos\phi_{\mathrm{T}}$	0.9
A_{SM}(k Yuan)	150	χ_{T}	0.2
A_{S}(k Yuan/kVA)	3	χ_{S}	0.6
$A_{\mathrm{CBCS,T}}$(k Yuan /kVA)	0.25	δ_{T}	0.75
A_{LI}(k Yuan/km)	1000	R_{AR}	1
Y_{CS}(Year)	20	M_{B}(kWh/m^2)	0.2
d	0.06	M_{SW}(m^2)	100
A_{BTV}(Yuan/km)	1.5	M_{C}(m^2)	25
M_{SM}(m^2)	100	$P_{\mathrm{SM,N}}$	50
$S_{i,j,\mathrm{MAX}}$(MVA)	2		

and Table I. The parameters and data in Fig. 7 and Table I in this article are from the Chinese reports and materials of China State Grid Corporation. Besides, with the development of science and technology, the price of battery materials decreases rapidly, and the market price of battery have already decreased to lower than 100 \$/kWh. And the latest reports, articles and webpages also confirm this point [52]–[54]. To verify the CBCS construction

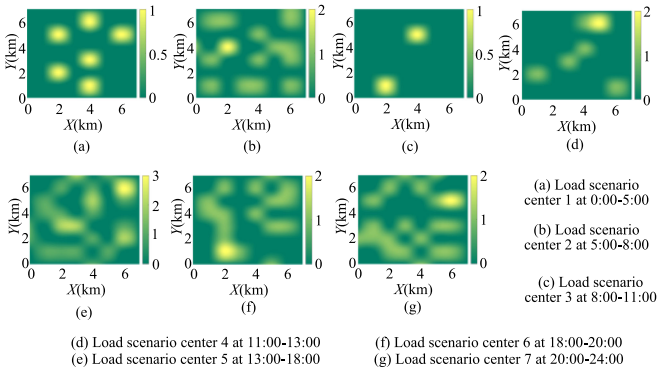

Fig. 8. Time-space load forecasting results of SEVs.

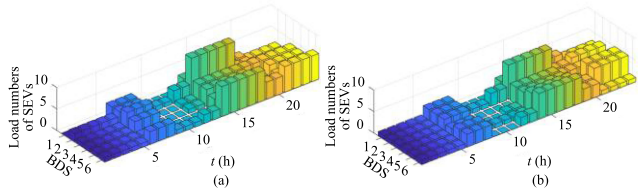

Fig. 9. SEV load of BDSs. (a) Case1/Case2. (b) Case3/Case4.

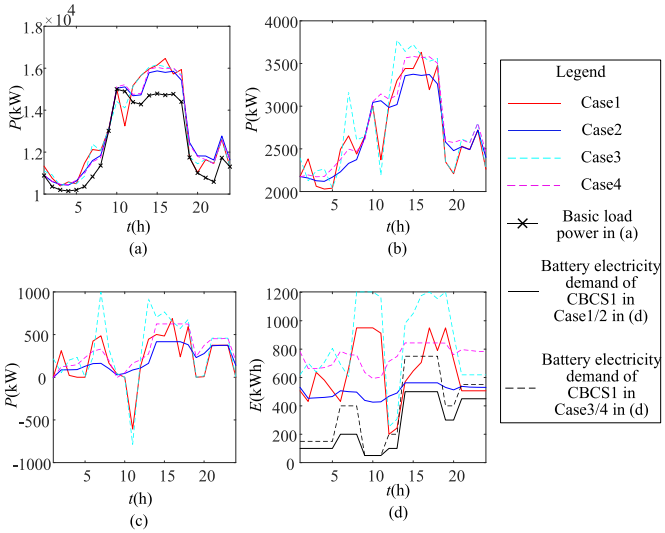

Fig. 10. Operation state of CBCS. (a) Load power of whole planning area. (b) Load power of substation 1. (c) Power of CBCS 1. (d) Energy storage level of CBCS 1.

quantities and whether it responds to the impact of grid dispatching on planning and operation, it is divided into four cases for comparative verification: cases 1 and 3 build three and two CBCSs, respectively, and CBCSs respond to grid dispatching; cases 2 and 4 build three and two CBCSs, respectively, and CBCSs do not respond to grid dispatching. Specifically, CBCS responds to grid dispatching, i.e., optimizing the power purchase cost of the grid while optimizing the objective function. If CBCS does not respond to grid dispatching, first remove the power purchase cost from the objective, then calculate and accumulate the power purchase cost into the objective after optimizing the planning. Based on case 3 (i.e., build two CBCSs, and CBCSs respond to grid dispatching), case 3-a is a single layer planning modeling and solving transformed from the double-level planning method proposed in this article, which is set to verify the feasibility and accuracy of the double-level planning model and double-loop iterative optimization method proposed in this article. That is, the cost objectives of lower and upper layers are accumulated to combine as a total planning cost, i.e., the single level objective. Then, a 0-1 integer programming is built to describe the shortest path optimization problem in the lower layer model (shown in Appendix A), which integrate into the upper layer planning model that transformed to an integral single level model. After that, the CPLEX toolbox is used to solve the single-level model. Furthermore, to verify the feasibility and accuracy of shortest path optimization in lower layer planning that solved by the BFA in this article. The classical shortest path algorithms, i.e., the Dijkstra algorithm [48] and Floyd algorithm [55] are used instead of the BFA to solve the lower layer planning of case 3, which are called case 3-b and case 1-c, respectively, (the upper layer planning is still optimized by CPLEX toolbox). Besides, the shortest path optimization result in case 3-a is also compared with case 3.

B. Case Analysis

The time-space load forecasting results of SEVs are shown in Fig. 8. And it can be seen from Fig. 8 that the load forecasting results reflect the time-space changing characteristic of SEVs, e.g., SPEVs load gathers in industrial and commercial areas, and SETs load gathers in a residential area at 5:00–8:00. And at 11:00–13:00, SPEVs and SETs both gather in industrial and commercial areas. Thus, the SEV forecasting method considers the driving and swapping habits of SEVs, and considers the randomness and uncertainty of driving distance, swapping time, and site of SEVs. Therefore, the SEV time-space load forecasting method proposed in this article is feasible. Afterward, SEVs load of each BDS is carried out, which shows in Fig. 9. As can be seen from Fig. 9, although the time-space load distribution of SEV in the planning area is the same, there are certain differences in the battery swapping demand load of BDS in different planning cases due to the different optimal locations of BDSs in cases 1, 2 and cases 3, 4. As a result, it improves the load analysis accuracy and planning rationality of CBCS.

Fig. 10 shows the optimized operation state of CBCS. It can be seen from Fig. 10(a) that cases 1 and 3 achieve a better grid operation economy, but the phenomenon of adding a peak load on the peak load will occur, and the peak-valley differences of the power grid reach 6079.31 and 5763.26 kW, respectively. Because the CBCS charge and discharge power of cases 1 and 3 are greatly affected by changes in baseload and real-time electricity price. However, the CBCS charge-discharge power scheme of cases 2, 4 is less affected by baseload and electricity price, so the peak-valley differences of the power grid are smaller, and the values are 5442.85 and 5593.95 kW, respectively. Then, it can be seen from Fig. 10(b) and (c) that the peak-valley differences and load fluctuation of cases 1 and 3 are greater than that of

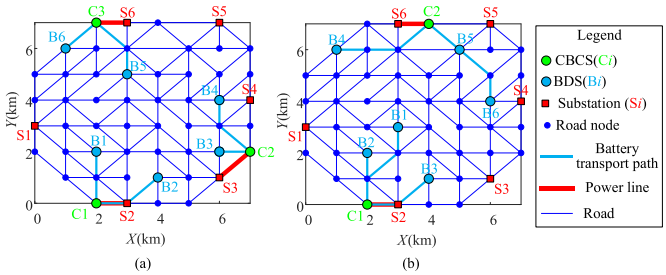

Fig. 11. Optimization results of locations of CBCSs and BDSs, and battery logistics path. (a) Case1/Case2. (b) Case3/Case4.

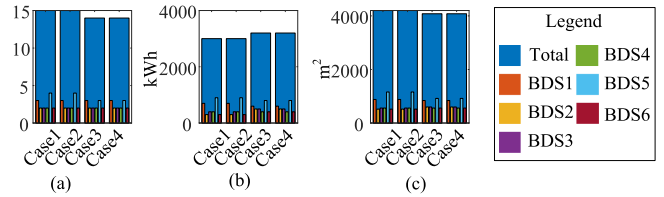

Fig. 12. Planning results of BDSs. (a) BDS swapper number. (b) BDS energy storage capacity. (c) BDS area.

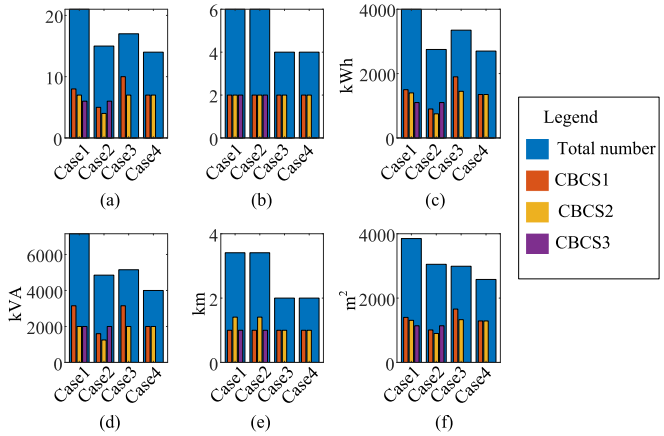

Fig. 13. Planning results of CBCSs. (a) CBCS charger number. (b) CBCS swapping equipment number. (c) CBCS energy storage capacity. (d) CBCS transformer capacity. (e) CBCS power line length. (f) CBCS area.

cases 2 and 4. Meanwhile, it can be seen from Fig. 10(b) and (c) that cases 1, 2 built 3 CBCSs, and cases 3 and 4 built 2 CBCSs, the power load of single CBCS of cases 1 and 2 is small, and the EV load increase to single grid substation is also small. Simultaneously, it can be seen from Fig. 10(d) that the operating electric quantity of CBCS of cases 1 to 4 is greater than the battery electric quantity demand of CBCS at any time. Therefore, from the analysis of the operation stage, it can be seen that the CBCS planning method and planning scheme in this article are feasible and effective. To sum up, the CBCS planning method proposed in this article considers and analyzes the operation stages of CBCS, which improves the rationality and accuracy of CSCS planning.

Fig. 11 shows the optimization results of locations of CBCSs and BDSs, and the battery logistics path. Figs. 12–14 show the planning results of BDSs, CBCSs, and substation expansion

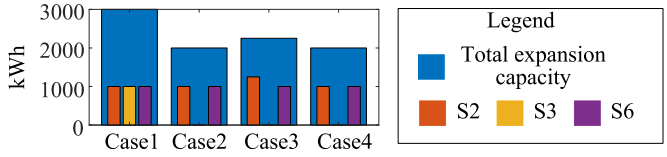

Fig. 14. Planning results of substation expansion capacity.

capacity. It can be seen from Fig. 11 that there is a strong coupling between the locations optimization of CBCSs, and BDSs, and the battery logistics system. Concurrently, cases 1 and 2 build 3 CBCSs, and cases 3 and 4 build 2 CBCSs. So, there are certain differences between the location scheme and battery logistics path between cases 1, 2 and cases 3, 4. The CBCSs and BDSs locations scheme and battery logistics path of cases 1 and 2 are the same, and the CBCSs and BDSs locations scheme and battery logistics path of cases 3 and 4 are the same. The CBCS and BDS planning method proposed in this article can better realize the planning of locations and scales (equipment quantity or capacity) of CBCSs and BDSs. Meanwhile, the battery logistics path is optimized, and the power lines of CBCSs are optimized. Simultaneously, the optimization results of substation capacity expansion are obtained. Therefore, the planning method proposed in this article has a high comprehensiveness.

It can be seen from Fig. 12(a)–(c) that with the decrease of CBCS amount from 3 to 2, the total swapper number and total area of BDSs both decreases, but the BDS energy storage capacity increase. This is because CBCS and BDS are both parts of SEV swapping and charging network, thus, the planning of CBCSs and BDSs has a strong coupling. With the decrease in CBCS amount, the utilization rates of BDS swappers and areas have been improved. But, it increases the battery supply uncertainties and volatilities of BDSs, and the transportation distance of batteries. So, it causes a certain increase in the energy storage capacity of BDS, e.g., in cases 1 and 3 (same operation states), the total swapper number and total area of BDS of case 3 are 1 and 120 m^2 less than those of case 1, respectively, but the BDS energy storage of case 3 is 200 kWh more than that of case 1. Meanwhile, it can be seen from Fig. 12(a)–(c) that the scale of each BDS is closely related to its SEV load, and satisfies the load demand of each BDS.

It can be seen from Fig. 13, under the same CBCS operation states (i.e., cases 1 and 3 or cases 2 and 4), with the decrease of CBCS amount from 3 to 2, and the total number of chargers, battery swapping equipment, energy storage capacity, transformer capacity, power line length, and area of CBCSs are reduced, e.g., the total number of chargers, battery swapping equipment, energy storage capacity, transformer capacity, power line length, and area of CBCSs of Case3 are 4, 2, 650 kWh, 2000 kVA, 1.41 km, and 860 m^2 less than those of case 1, respectively. It shows that with the reduction of CBCS build number, the equipment utilization rate of CBCS is greatly improved. Moreover, it can be seen from Fig. 13 that the scales of CBCSs are closely related to the load of BDS for energy supply, and meets the battery demand of BDSs for energy supply. Concurrently, it can be seen from Fig. 14 that due to the reduction of the

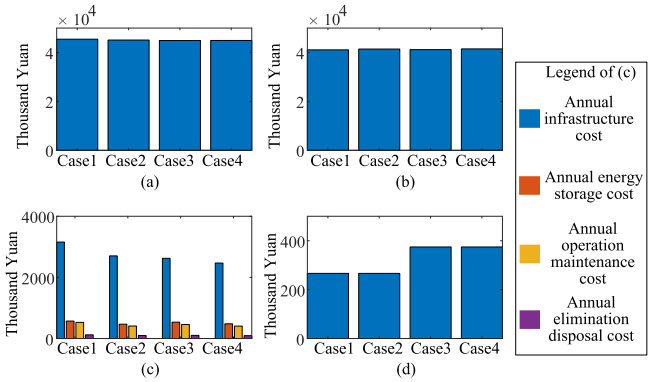

Fig. 15. Each planning cost. (a) Annual comprehensive cost. (b) Annual energy purchase cost. (c) Other annual costs. (d) Annual transportation cost of battery logistics company.

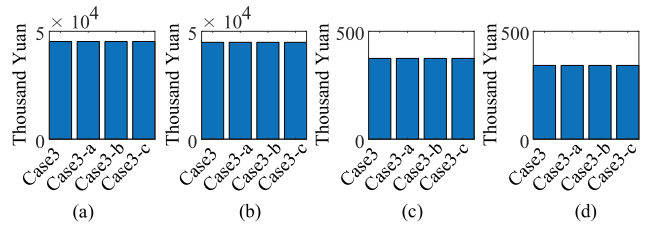

Fig. 16. Planning results of different models and solving methods. (a) Total planning cost. (b) Annual comprehensive cost. (c) Annual transportation cost of battery logistics company. (d) Total transport mileage of BTVs.

scale of CBCSs, the expansion capacities of substations are also reduced, e.g., the substation expansion capacity of case 3 is 750 kVA less than that of case1. To sum up, with the decrease in CBCS amount, the scales of CBCSs, BDSs, and substations are reduced.

Fig. 15 shows each planning cost. It can be seen from Fig. 15 that under the same CBCS operation states (i.e., cases 1 and 3 or cases 2 and 4), with the decrease of CBCS amount from 3 to 2, the planning costs of annual comprehensive, energy purchase, infrastructure, energy storage, operation maintenance, and elimination disposal have decreased, while the annual cost of the battery logistics company has increased. Case 3 has the lowest annual comprehensive cost, which is 560.37, 206.40, 32.71 thousand Yuan lower than those of cases 1, 2, and 4, respectively. The annual infrastructure cost of case 3 is 531.83, 80.21, and -154.10 thousand Yuan lower than those of cases 1, 2, and 4, respectively. Then, the annual energy purchase cost of case 3 is -94.84, 245.94, 302.35 thousand Yuan lower than those of cases 1, 2, and 4, respectively. The differences in other costs are small. And the annual battery logistics company cost of case 3 is 108.01 thousand Yuan higher than cases 1 and 2 and the same as that of case 4. Fig. 16 shows the planning results of different models and solving methods. From Fig. 16(a)–(d), it can be seen that there are no differences between the optimization results of double-level optimization planning of case 3 in this article and single-level modeling and solving of case 3-a. As a result, the feasibilities and accuracies of the double-level planning model and double-loop iterative optimization method developed in this article are verified. In addition, through the comparison among case 3, case 3-a, case 3-b, and case 3-c, it can be seen that the optimization results of BFA, Dijkstra algorithm, Floyd algorithm, and 0-1 integer programming method for shortest path problem are the same. It well verifies the feasibility and accuracy of BFA to optimize the shortest driving paths of BTVs in the lower layer planning of this article.

To sum up, case 3 has great advantages in the planning construction scale and overall economy of the battery charging and swapping network. Thus, case 3 is finally selected as the final planning scheme for construction.

VII. Conclusion

This article presents a planning method for CBCSs and BDSs taking into account the battery logistics system. First, a time-space load forecasting model of SEVs is built. Secondly, operation models of CBCS, BDS, and the battery logistics system are built. Then, sizing models of CBCSs and BDSs are established. Finally, a double-level planning model of CBCSs considering battery logistics system is proposed. In conclusion, the planning method proposed in this article is feasible and effective. The results are shown that the following.

1) The time-space load forecasting results reflect the time-space changing characteristic of SEVs. The SEV forecasting method proposed thinks over the different driving habits and battery swapping habits of different types SEVs (e.g., SPEVs and SETs) users. Simultaneously, this forecasting method considers the randomness and uncertainty of driving distance, swapping time, location, etc. Therefore, the SEV time-space load forecasting method in this article is feasible, and it improves the planning rationality of CBCS.
2) The CBCS and BDS planning method thinking over the battery logistics system proposed in this article can realize the planning of scales and locations of CBCSs and BDSs better. Meanwhile, the battery logistics path, CBCS power lines, and substation expansion are optimized. Concurrently, the planning method takes into account the operation stages of CBCSs, BDSs, and the battery logistics system. At the same time, the planning of CBCS and BDS has a strong coupling. With the decrease in CBCS amount, the scales of CBCSs, BDSs, and substations are reduced. Thus, the planning economy is improved.

Appendix A

The road network of the planning area is represented by an undirected weighted connectivity graph $\boldsymbol{G}_R = (\boldsymbol{V}_R, \boldsymbol{E}_R)$. Where, $\boldsymbol{V}_R$ is the road node set, and $\boldsymbol{E}_R$ is the connection set of road nodes. It is assumed that there is only one feasible path between two adjacent road nodes at most. $W_{R,i,j}$ is the length between road nodes, and the length matrix is $\boldsymbol{W}_R(W_{R,i,j} \in \boldsymbol{W}_R, \forall i, j)$. The ST means source node, and DE means destination node. The binary constant $K_{\mathrm{R},i,j}$ represent

connection status of road nodes, which satisfies

$$K_{R,i,j}=\begin{cases}1, \text{It has path between node } i \text{ and node } j\\ 0, \text{It does not have path between node } i \text{ and node } j\end{cases}. \tag{A1}$$

Furthermore, the 0-1 integer programming is built to describe the shortest path optimization problem, which satisfies (A2) to (A4)

$$F_{\text{Path}}=\sum_{i=S}^{\text{DE}}\sum_{\substack{i=S\\ j\neq i}}^{\text{DE}}\left(W_{R,i,j}K_{R,i,j}\right) \tag{A2}$$

$$\text{s.t.}\sum_{\substack{j=\text{ST}\\ j\neq i}}^{\text{DE}}K_{i,j}-\sum_{\substack{j=\text{ST}\\ j\neq i}}^{\text{DE}}K_{j,i}=\begin{cases}1, i=\text{ST}\\ -1, i=\text{DE}\\ 0, \text{others}\end{cases} \tag{A3}$$

$$\begin{cases}\sum\limits_{\substack{j=\text{ST}\\ j\neq i}}^{\text{DE}}K_{i,j}\leq 1, i\neq \text{DE}\\ \sum\limits_{\substack{j=\text{ST}\\ j\neq i}}^{\text{DE}}K_{i,j}=0, i=\text{DE}\end{cases}, K_{i,j}\in\{0,1\}\ \forall i. \tag{A4}$$

REFERENCES

[1] C. He, J. Zhu, S. Li, Z. Chen, and W. Wu, "Sizing and locating planning of EV centralized-battery-charging-station considering battery logistics system," in *Proc. IEEE 4th Int. Elect. Energy Conf.*, 2021, pp. 1–6.

[2] K. Qian, C. Zhou, M. Allan, and Y. Yuan, "Modeling of load demand due to EV battery charging in distribution systems," *IEEE Trans. Power Syst.*, vol. 26, no. 2, pp. 802–810, May 2011.

[3] S. Bae and A. Kwasinski, "Spatial and temporal model of electric vehicle charging demand," *IEEE Trans. Smart Grid*, vol. 3, no. 1, pp. 394–403, Mar. 2012.

[4] O. Hafez and K. Bhattacharya, "Queuing analysis based PEV load modeling considering battery charging behavior and their impact on distribution system operation," *IEEE Trans. Smart Grid*, vol. 9, no. 1, pp. 261–273, Jan. 2018.

[5] Y. Mu, J. Wu, N. Jenkins, H. Jia, and C. Wang, " A spatial–temporal model for grid impact analysis of plug-in electric vehicles," *Appl. Energy*, vol. 114, no. 1, pp. 456–465, 2014.

[6] W. Yang, Y. Xiang, J. Liu, and C. Gu, "Agent-based modeling for scale evolution of plug-in electric vehicles and charging demand," *IEEE Trans. Power Syst.*, vol. 33, no. 2, pp. 1915–1925, Mar. 2018.

[7] K. Chaudhari, N. K. Kandasamy, A. Krishnan, A. Ukil, and H. B. Gooi, "Agent-based aggregated behavior modeling for electric vehicle charging load," *IEEE Trans. Ind. Informat.*, vol. 15, no. 2, pp. 856–868, Feb. 2019.

[8] S. Shahidinejad, S. Filizadeh, and E. Bibeau, "Profile of charging load on the grid due to plug-in vehicles," *IEEE Trans. Smart Grid*, vol. 3, no. 1, pp. 135–141, Mar. 2012.

[9] N. Ghiasnezhad Omran and S. Filizadeh, "Location-based forecasting of vehicular charging load on the distribution system," *IEEE Trans. Smart Grid*, vol. 5, no. 2, pp. 632–641, Mar. 2014.

[10] M. Majidpour, C. Qiu, P. Chu, R. Gadh, and H. R. Pota, "Fast prediction for sparse time series: Demand forecast of EV charging stations for cell phone applications," *IEEE Trans. Ind. Informat.*, vol. 11, no. 1, pp. 242–250, Feb. 2015.

[11] Q. Dai, T. Cai, S. Duan, and F. Zhao, "Stochastic modeling and forecasting of load demand for electric bus battery-swap station," *IEEE Trans. Power Del.*, vol. 29, no. 4, pp. 1909–1917, Aug. 2014.

[12] M. Dabbaghjamanesh, A. Moeini, and A. Kavousi-Fard, "Reinforcement learning-based load forecasting of electric vehicle charging station using Q-learning technique," *IEEE Trans. Ind. Informat.*, vol. 17, no. 6, pp. 4229–4237, Jun. 2021.

[13] M. Alizadeh, A. Scaglione, J. Davies, and K. S. Kurani, "A scalable stochastic model for the electricity demand of electric and plug-in hybrid vehicles," *IEEE Trans. Smart Grid*, vol. 5, no. 2, pp. 848–860, Mar. 2014.

[14] X. Zhang, K. W. Chan, H. Li, H. Wang, J. Qiu, and G. Wang, "Deep-learning-based probabilistic forecasting of electric vehicle charging load with a novel queuing model," *IEEE Trans. Cybern.*, vol. 51, no. 6, pp. 3157–3170, Jun. 2021.

[15] M. F. Shaaban, S. Mohamed, M. Ismail, K. A. Qaraqe, and E. Serpedin, "Joint planning of smart EV charging stations and DGs in eco-friendly remote hybrid microgrids," *IEEE Trans. Smart Grid*, vol. 10, no. 5, pp. 5819–5830, Sep. 2019.

[16] X. Wang, M. Shahidehpour, C. Jiang, and Z. Li, "Coordinated planning strategy for electric vehicle charging stations and coupled traffic-electric networks," *IEEE Trans. Power Syst.*, vol. 34, no. 1, pp. 268–279, Jan. 2019.

[17] S. Wang, Z. Y. Dong, F. Luo, K. Meng, and Y. Zhang, "Stochastic collaborative planning of electric vehicle charging stations and power distribution system," *IEEE Trans. Ind. Informat.*, vol. 14, no. 1, pp. 321–331, Jan. 2018.

[18] B. Zeng, H. Dong, F. Xu, and M. Zeng, "Bilevel programming approach for optimal planning design of EV charging station," *IEEE Trans. Ind. Appl.*, vol. 56, no. 3, pp. 2314–2323, May/Jun. 2020.

[19] H. Zhang, S. J. Moura, Z. Hu, and Y. Song, "PEV fast-charging station siting and sizing on coupled transportation and power networks," *IEEE Trans. Smart Grid*, vol. 9, no. 4, pp. 2595–2605, Jul. 2018.

[20] A. Ehsan and Q. Yang, "Active distribution system reinforcement planning with EV charging stations–part II: Numerical results," *IEEE Trans. Sustain. Energy*, vol. 11, no. 2, pp. 979–987, Apr. 2020.

[21] N. Bañol Arias, A. Tabares, J. F. Franco, M. Lavorato, and R. Romero, "Robust joint expansion planning of electrical distribution systems and EV charging stations," *IEEE Trans. Sustain. Energy*, vol. 9, no. 2, pp. 884–894, Apr. 2018.

[22] I. S. Bayram, A. Tajer, M. Abdallah, and K. Qaraqe, "Capacity planning frameworks for electric vehicle charging stations with multiclass customers," *IEEE Trans. Smart Grid*, vol. 6, no. 4, pp. 1934–1943, Jul. 2015.

[23] L. Ni, B. Sun, X. Tan, and D. H. K. Tsang, "Inventory planning and real-time routing for network of electric vehicle battery-swapping stations," *IEEE Trans. Transp. Electrific.*, vol. 7, no. 2, pp. 542–553, Jun. 2021.

[24] Y. Zheng, Z. Y. Dong, Y. Xu, K. Meng, J. H. Zhao, and J. Qiu, "Electric vehicle battery charging/swap stations in distribution systems: Comparison study and optimal planning," *IEEE Trans. Power Syst.*, vol. 29, no. 1, pp. 221–229, Jan. 2014.

[25] S. Wang, L. Yu, L. Wu, Y. Dong, and H. Wang, "An improved differential evolution algorithm for optimal location of battery swapping stations considering multi-type electric vehicle scale evolution," *IEEE Access*, vol. 7, pp. 73020–73035, 2019.

[26] X. Liu and Z. Bie, "Cooperative planning of distributed renewable energy assisted 5G base station with battery swapping system," *IEEE Access*, vol. 9, pp. 119353–119366, 2021.

[27] M. Ban, D. Guo, J. Yu, and M. Shahidehpour, "Optimal sizing of PV and battery-based energy storage in an off-grid nanogrid supplying batteries to a battery swapping station," *J. Modern Power Syst. Clean Energy*, vol. 7, no. 2, pp. 309–320, Mar. 2019.

[28] Y. Wang, Y. Yang, N. Zhang, and M. Huang, "An integrated optimization model of charging station/battery-swap station/energy storage system considering uncertainty," in *Proc. IEEE Int. Conf. Energy Internet*, 2017, pp. 77–82.

[29] H. Gan and C. Zheng, "An optimization model for capacity planning and ordered discharging of centralized charging stations," in *Proc. 2nd IEEE Conf. Energy Internet Energy Syst. Integration (EI2)*, 2018, pp. 1–9.

[30] Q. Kang, J. Wang, M. Zhou, and A. C. Ammari, "Centralized charging strategy and scheduling algorithm for electric vehicles under a battery swapping scenario," *IEEE Trans. Intell. Transp. Syst.*, vol. 17, no. 3, pp. 659–669, Mar. 2016.

[31] W. Zhong, K. Xie, Y. Liu, C. Yang, S. Xie, and Y. Zhang, "Dynamic scheduling of multi-type battery charging stations for EV battery swapping," in *Proc. IEEE Int. Conf. Commun., Control, Comput. Technol. Smart Grids (SmartGridComm)*, 2019, pp. 1–6.

[32] W. Tao *et al.*, "Integrated optimal configuration of electric vehicle charging and battery-swapping station based on ordered charging strategy," in *Proc. China Int. Conf. Electricity Distrib.*, 2018, pp. 2237–2241.

[33] L. Yongxiang, X. Ruilin, C. Tao, Z. Xiaoyong, W. Ruimiao, and Y. Xi, "Investigation on the construction mode of the charging station and battery-swap station," in *Proc. Int. Conf. Elect. Inf. Control Eng.*, 2011, pp. 5080–5081.

[34] Y. Deng, Y. Zhang, F. Luo, and Y. Mu, "Operational planning of centralized charging stations utilizing second-life battery energy storage systems," *IEEE Trans. Sustain. Energy*, vol. 12, no. 1, pp. 387–399, Jan. 2021.
[35] X. Zhang and G. Wang, "Optimal dispatch of electric vehicle batteries between battery swapping stations and charging stations," in *Proc. IEEE Power Energy Soc. Gen. Meeting*, 2016, pp. 1–5.
[36] X. Tan, G. Qu, B. Sun, N. Li, and D. H. K. Tsang, "Optimal scheduling of battery charging station serving electric vehicles based on battery swapping," *IEEE Trans. Smart Grid*, vol. 10, no. 2, pp. 1372–1384, Mar. 2019.
[37] A. Relan, V. Gupta, R. Kumar, S. Vyas, and B. K. Panigrahi, "Optimal siting of electric vehicle battery swapping stations with centralized charging," in *Proc. IEEE Int. Conf. Power Electron., Drives Energy Syst.*, 2020, pp. 1–6.
[38] M. Moradijoz, M. Parsa Moghaddam, and M. Haghifam, "A flexible distribution system expansion planning model: A dynamic bi-level approach," *IEEE Trans. Smart Grid*, vol. 9, no. 6, pp. 5867–5877, Nov. 2018.
[39] Y. Zhao, Y. Guo, Q. Guo, H. Zhang, and H. Sun, "Deployment of the electric vehicle charging station considering existing competitors," *IEEE Trans. Smart Grid*, vol. 11, no. 5, pp. 4236–4248, Sep. 2020.
[40] X. Duan, Z. Hu, Y. Song, K. Strunz, Y. Cui, and L. Liu, "Planning strategy for an electric vehicle fast charging service provider in a competitive environment," *IEEE Trans. Trans. Electrific.*, to be published, doi: 10.1109/TTE.2022.3152387.
[41] C. Lei, L. Lu, and Y. Ouyang, "System of systems model for planning electric vehicle charging infrastructure in intercity transportation networks under emission consideration," *IEEE Trans. Intell. Trans. Syst.*, to be published, doi: 10.1109/TITS.2021.3076008.
[42] B. Zeng, H. Dong, F. Xu, and M. Zeng, "Bilevel programming approach for optimal planning design of EV charging station," *IEEE Trans. Ind. Appl.*, vol. 56, no. 3, pp. 2314–2323, May/Jun. 2020.
[43] B. Zeng, H. Dong, R. Sioshansi, F. Xu, and M. Zeng, "Bilevel robust optimization of electric vehicle charging stations with distributed energy resources," *IEEE Trans. Ind. Appl.*, vol. 56, no. 5, pp. 5836–5847, Sep./Oct. 2020.
[44] F. E. Moore, "The shortest path through a maze," in *Proc. Int. Symp. Theory Switching*, 1959, pp. 285–292.
[45] L. Thibault, G. De Nunzio, and A. Sciarretta, "A unified approach for electric vehicles range maximization via eco-routing, eco-driving, and energy consumption prediction," *IEEE Trans. Intell. Veh.*, vol. 3, no. 4, pp. 463–475, Dec. 2018.
[46] C. De Cauwer, W. Verbeke, J. Van Mierlo, and T. Coosemans, "A model for range estimation and energy-efficient routing of electric vehicles in real-world conditions," *IEEE Trans, Intell. Transp. Syst.*, vol. 21, no. 7, pp. 2787–2800, Jul. 2020.
[47] R. Bellman, "On a routing problem," *Quart. Appl. Math.*, vol. 16, no. 1, pp. 87–90, 1958.
[48] P. M. Ismael, H. Y. Ibrahim, and A. B. Al-Khalil, "A real time parking reservation system based on vehicular cloud computing," in *Proc. Int. Conf. Comput. Sci. Softw. Eng.*, 2020, pp. 26–31, doi: 10.1109/CSASE48920.2020.9142122.
[49] Z. Fan *et al.*, "Multi-objective planning of DGs considering ES and EV based on source-load spatiotemporal scenarios," *IEEE Access*, vol. 8, pp. 216835–216843, 2020.
[50] X. Huang, Y. Ye, and H. Zhang, "Extensions of kmeans-type algorithms: A new clustering framework by integrating intracluster compactness and intercluster separation," *IEEE Trans. Neural Netw. Learn. Syst.*, vol. 25, no. 8, pp. 1433–1446, Aug. 2014.
[51] L. Gong, W. Cao, and J. Zhao, "Load modeling method for EV charging stations based on trip chain," in *Proc. IEEE Conf. Energy Internet Energy Syst. Integration*, 2017, pp. 1–5.
[52] G. Pan, W. Gu, Y. Lu, H. Qiu, S. Lu, and S. Yao, "Optimal planning for electricity-hydrogen integrated energy system considering power to hydrogen and heat and seasonal storage," *IEEE Trans. Sustain. Energy*, vol. 11, no. 4, pp. 2662–2676, Oct. 2020.
[53] Average cost of lithium-ion battery cell below $100 kWh in 2023, Accessed: Sep. 24, 2020. [Online]. Available: https://www.pveurope.eu/solar-storage/average-cost-lithium-ion-battery-cell-below-100-kwh-2023
[54] Average Cost of Lithium-ion Battery Cell Likely to Plummet to $100/kWh in 2023: Report, Accessed: Sep. 25, 2020. [Online]. Available: https://mercomindia.com/average-cost-lithium-ion-battery/
[55] Y. Deng, Y. Mu, X. Dong, H. Jia, J. Wu, and S. Li, "Hierarchical operation management of electric vehicles for depots with PV on-site generation," *IEEE Trans. Smart Grid*, vol. 13, no. 1, pp. 641–653, Jan. 2022.

Chenke He was born in Zhejiang, China in 1993. He received the B.S. degree in electrical engineering from the Henan University of Technology, Henan, China, in 2016, and the M.S. degree in electrical engineering from the Shanghai University of Electric Power, Shanghai, China, in 2019. He is currently working toward the Ph.D. degree in electrical engineering with the School of Electric Power Engineering, South China University of Technology, Guangzhou, China.

His current research interests include the optimization planning of electric vehicle charging and swapping facilities as well as integrated energy system.

Jizhong Zhu (Fellow, IEEE) was born in Sichuan, China in 1966. He received the B.S., M.S., and Ph.D. degrees in electrical engineering from Chongqing University, Chongqing, China, in 1985, 1987, and 1990, respectively.

His work experience includes Chongqing University; Brunel University, U.K.; National University of Singapore; Howard University; ALSTOM Grid Inc., and SEPRI, CSG. He is currently a Professor with the School of Electric Power Engineering, South China University of Technology. His research interests include power system operation and control, smart grid, microgrid, virtual power plant, electric vehicle, renewable energy application and integrated smart energy system.

Shenglin Li received the B.S. and M.S. degrees from Shanghai University of Electric Power, Shanghai, China, in 2016 and 2019, respectively. He is currently working toward the Ph.D. degree in electrical engineering with the School of Electric Power Engineering, South China University of Technology, Guangzhou, China.

His current research interests include the energy management of renewable energy microgrids as well as energy trading.

Ziyu Chen received the B.S. degree in electrical engineering from Guangdong University of Technology, Guangzhou, China, in 2017. She is currently working toward the Ph.D. degree in electrical engineering with the School of Electric Power Engineering, South China University of Technology, Guangzhou, China.

Her current research interests include cyber physical social systems, operation and control of smart energy system and cyber-attack detection.

Wanli Wu received the B.S. and M.S. degrees in electrical engineering from Guangdong University of Technology, Guangzhou, China, in 2017 and 2020. She is currently working toward the Ph.D. degree in electrical engineering with the School of Electric Power Engineering, South China University of Technology, Guangzhou, China.

Her research interests include electric vehicle to grid and game theory.